Journal of Solid State Chemistry 183 (2010) 1741–1746

Contents lists available at ScienceDirect

Journal of Solid State Chemistry

journal homepage: www.elsevier.com/locate/jssc

Structural studies of the disorder and phase transitions in the double perovskite Sr_2YTaO_6

Qingdi Zhou [a], Brendan J. Kennedy [a,*], Maxim Avdeev [b]

[a] School of Chemistry, The University of Sydney, Sydney, NSW 2006, Australia
[b] Bragg Institute, Australian Nuclear Science and Technology Organisation, Private Mail Bag 1, Menai, NSW 2234, Australia

ARTICLE INFO

Article history:
Received 26 March 2010
Received in revised form
13 May 2010
Accepted 17 May 2010
Available online 2 July 2010

Keywords:
Perovskite
Phase transition
Cation disorder

ABSTRACT

The evolution of the crystal structure of the double perovskite Sr_2YTaO_6 from room temperature to 1250 °C has been studied using powder neutron and synchrotron X-ray diffraction. At room temperature Sr_2YTaO_6 crystallises in a monoclinic superstructure with the space group $P2_1/n$. The tilting of the octahedra evident in the room temperature structure is progressively lost on heating, resulting in a sequence of phase transitions that ultimately yields the cubic structure in space group $Fm\bar{3}m$. The high temperature tetragonal and cubic phases are characterised by strongly anisotropic displacements of the anions. The amount of defects in the crystal structure of Sr_2YTaO_6 is found to be sensitive to the preparative method.

1. Introduction

Perovskites are an important class of materials employed in a number of technological applications, including microwave resonators, solid oxide fuel cells, catalysis, and sensors [1–3]. The physical and chemical characteristics of ABO_3 oxide perovskites are closely correlated to the identity and coordination environment of the octahedral *B*-site cation. Changes in this cation impact on the important structural characteristics, such as deformation/tilting of BO_6 octahedra and the electronic and magnetic properties of the materials [4]. The choice of *B*-site cation is therefore of crucial importance for the rational design and optimisation of perovskites for specific applications [5,6].

A common approach to tune the structure and, hence, properties of ABO_3 perovskites is substitution of the cation at the octahedral site forming oxides of the type, $AB_{1-x}B'_xO_3$. In situations where $x \sim 0.5$ and when the size and/or charge of these two cations are sufficiently different the materials exhibit a 1:1 ordering of the two *B*-site cations, with alternating layers of the *B* and *B*′ cations along the [111] axis of the cubic perovskite cell, leading to a doubling of the unit cell lattice parameter [7]. This three-dimensional arrangement of the *B* and *B*′ cations yields the same topology as that of the anions and cations in the NaCl "rock-salt" structure. Consequently, this type of ordering is often called the rock-salt-type ordering.

The inclusion of small d^0 cations, such as Ta^{5+}, Nb^{5+}, and Ti^{4+}, on the *B*-site in complex perovskites such as $BaB_{1/3}Ta_{2/3}O_3$ (B=Mg, Zn) can result in attractive dielectric properties [6]. In general, such perovskites adopt centrosymmetric structures and, consequently, they are not ferroelectrics. Nevertheless, in selected cases, electronic polarisation results in relatively large dielectric permittivities. It has been found that the dielectric behaviour of complex perovskites can vary significantly depending upon the extent of both cation ordering and octahedral tilting. Empirically, lower dielectric losses have been associated with higher degrees of cation ordering, while the more negative resonant frequencies are associated with the absence of tilting of the octahedral moieties [8,9].

While the topology (the arrangement of atoms) of the perovskite structure is thermodynamically extremely stable, the actual crystal structure (the position of the atoms) is very flexible [9]. Another feature of the many perovskites is a high degree of pseudo-symmetry [10]. This presents challenges in establishing the precise crystal structure of a given material, but also makes them excellent candidates for the observation of structural phase transitions which can, in turn, be related to their physical properties.

In continuation of our previous work on cation ordered double perovskites [11–13] we report here the synthesis, crystal symmetries, and high temperature structural phase transitions in the ordered double perovskite Sr_2YTaO_6.

2. Experimental

Commercially available materials $SrCO_3$ (Aldrich ≥99.9%), Y_2O_3 (Merck, ≥99%), Ta_2O_5 (Aldrich, 99.99%) were utilised in the

* Corresponding author. Fax: +61 2 9351 3329.
E-mail address: b.kennedy@chem.usyd.edu.au (B.J. Kennedy).

0022-4596/$ - see front matter © 2010 Elsevier Inc. All rights reserved.
doi:10.1016/j.jssc.2010.05.018

synthesis. These were dried overnight before use. Sr_2YTaO_6 powder was synthesised by two methods. The first was a conventional solid state method using $YTaO_4$[1] and $SrCO_3$. These were mixed using a mortar and pestle and then heated at 1400 °C for 3 days with intermittent regrinding. The second method used in the preparation was similar to that described in Ref. [14]. Stoichiometric amounts of $SrCO_3$, Y_2O_3, and Ta_2O_5 were ball milled in distilled water for 48 h. The slurry was dried and mixed with 0.5 wt% Nb_2O_5, as a sintering aid, and then pelletized. The pellets were heated at 600 °C for 30 min and 1600 °C for 4 h. After annealing all samples were furnace cooled to room temperature at about 5 °C/min. Both samples were reground and X-rayed between heating steps using a PANalytical X'Pert PRO MPD. High temperature X-ray diffraction data were collected for the conventionally prepared sample using a Panalytical X'Pert Pro X-ray diffractometer equipped with a Real Time Multiple Strip (RTMS) X'celerator detector covering a solid angular range of 2° at 25 °C employing Cu$K\alpha$ radiation and Anton Parr HTK16 hot stage.

Raman spectra were recorded on a Renishaw Raman inVia Reflex spectrometer using Leica DMLM microscope with objective of 20× for the room temperature measurements. The scattered light is collected (180° backscattering geometry) along the same optical path as the incoming laser. An Ar^+ laser (Modu-Laser, UT, USA) of 514 nm with effective 2.6 mW power at the sample surface was used as the exciting line. A liquid N_2-cooled charge coupled device (CCD) with a grating 2400 l/mm detected the scattered light. The accumulation time for one collection was 30 s.

Neutron powder diffraction data of the conventionally prepared polycrystalline sample of Sr_2YTaO_6 were measured using the high resolution powder diffractometer, Echidna, at the OPAL facility (Australian Nuclear Science and Technology Organisation) at a wavelength of 1.622 Å [15]. For these measurements the sample was contained in a cylindrical vanadium can that was mounted in a vacuum furnace. The diffraction data were collected between room temperature and 1200 °C at 100 °C steps. For each measurement the temperature was equilibrated for 20 min before collecting data for 4 h. The synchrotron X-ray diffraction data were collected for both samples at ambient temperature in the angular range $5 < 2\theta < 85°$, using X-rays of wavelength 0.82465 Å on the powder diffractometer at BL-10 of the Australian Synchrotron [16]. The samples were housed in 0.3 mm diameter capillaries that were rotated during the measurements. The structures were refined using the program RIETICA [17]. The peak shapes were modelled using a pseudo-Voigt function and the background was estimated by interpolating between up to 40 selected points.

3. Results and discussion

Two samples of Sr_2YTaO_6 were prepared, the first using a conventional solid state method that involved several heating stages. In the second, the constituent materials were initially treated in a planetary ball mill and heated for a much shorter period. The ball mill method utilised here is commonly employed in studies of the microwave dielectric properties of such oxides, where the preparation of dense single phase samples is critical. Laboratory X-ray diffraction data showed both methods yield essentially single phase Sr_2YTaO_6. The synchrotron X-ray diffraction data confirmed both the rock salt-type ordering of the Y^{3+} and Ta^{5+} cations and monoclinic symmetry described in our previous work [18]. The data of the conventionally prepared sample were fitted to a model in space group $P2_1/n$ (Fig. 1) and the refined structural parameters from this fit, and from fitting of the powder neutron diffraction data, are tabulated in Table 1 and are in a good agreement with the previous studies [18]. Selected bond distances are given in Table 2.

However, as is evident from Fig. 2, the Rietveld fit to the synchrotron data of the sample prepared using the ball mill is less than optimal ($\chi^2=4.7\%$), although a LeBail type analysis provided an acceptable fit to the data ($\chi^2=2.4\%$). Attempts to model the synchrotron diffraction data from the ball milled sample with a triclinic model failed to significantly improve the quality of the Rietveld fit over that in the monoclinic model indicating that this poor fitting is not due to a lowering of symmetry. Likewise effects such as preferred orientation (which appears to be small) and anisotropic peak-broadening did not provide a satisfactory model to the data. Examination of the difference profiles show that the intensities of some reflections are underestimated, whereas others are overestimated. This shows that the model does not adequately reproduce the electron density (atomic positions and site occupancies) of the unit cell. Such discrepancies are seen in a number of double perovskites and are often modelled by "anti-site" disorder in which some of the B is placed on the B' sites and vice-versa [9,19]. Since the average Ta–O and Y–O bond distances are very different in Sr_2YTaO_6 (see Table 3), we did not attempt to fit the data using an anti-site disorder model. Ting et al. [20] argued that for Ba_2InNbO_6 the anti-site disorder actually corresponds to fine scale translational stacking faults. We found that we could model the data for the ball milled sample using a 2-phase monoclinic model in which only the lattice parameters of the second phase were refined, that is the TaO_6 and YO_6 coordination in both phases is identical. This provided an excellent fit to the observed data with $\chi^2=3.3\%$. It is possible that the local disorder/stacking faults that are responsible for the observed broadening of the peaks will impact on the electronic polarisation and hence dielectric permittivities.

Further evidence for the presence of local disorder comes from the Raman spectra of the two samples. There are a number of subtle differences between the Raman spectra of the samples prepared using the two methods with the ball milled sample exhibiting a number of extra lines (Fig. 3). Superficially the spectra are very similar to that presented by Dias et al. [14] and the reader is referred to this earlier work for possible assignments of the various modes. Of interest, however, is the broadening of the Raman lines in the ball milled sample compared with the lines in the conventionally prepared sample. This suggests the phonon lifetimes are shorter in the former sample, indicating this contains an increased number of structural defects or disorder. This is despite the high temperature (1600 °C) anneal that the sample had been subjected to post ball-milling. The second feature of interest is the small number of additional lines in the spectrum of the ball milled sample. Since the diffraction data do not provide any evidence for the presence of secondary phases in this sample, these additional lines probably indicate a lowering of local symmetry. Recall that the model used to reproduce the synchrotron pattern has two identical structures, with slightly different lattice parameters; this model should not result in the presence of any additional Raman modes. The most probable symmetry lowering process is partial disorder of the Ta^{5+} and Y^{3+} cations in the octahedral sites. Dias et al. [21,22] postulated such effects are present in the analogous Ba compound Ba_2YNbO_6, although in that case they proposed the presence of a triclinic phase. As noted above our diffraction data do not require we use a lower symmetry model, but the variation in intensities does

[1] $YTaO_4$ was prepared by heating Y_2O_3 and Ta_2O_5 at 800 °C for12 h, and then between 1100 and 1400 °C for 2 weeks until a single phase is obtained.

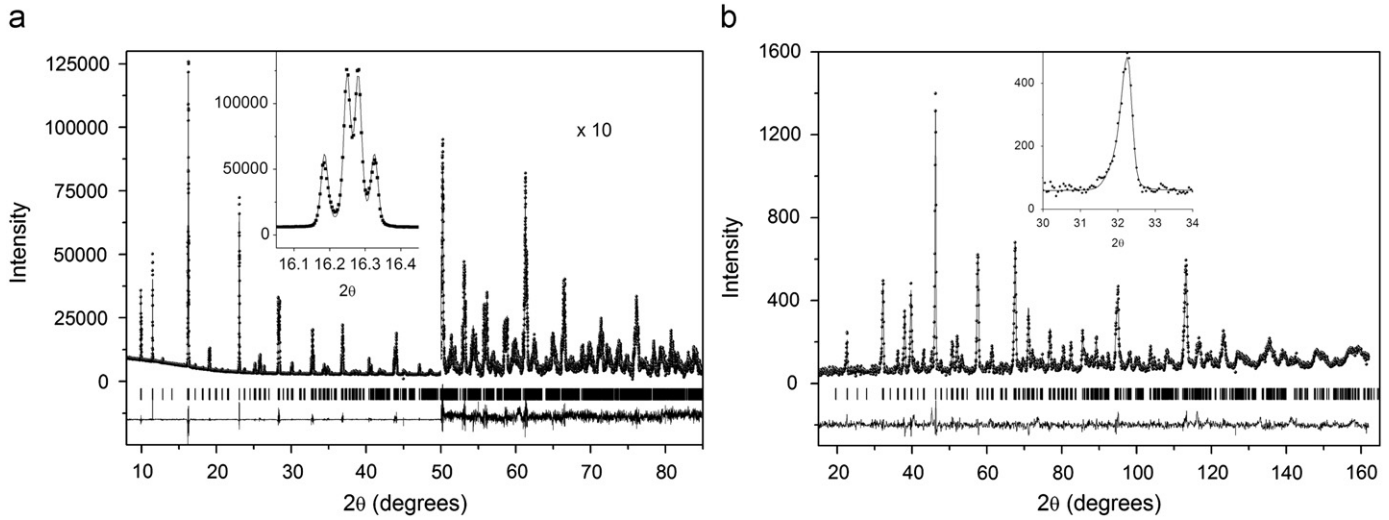

Fig. 1. (a) Synchrotron X-ray powder diffraction profiles for Sr_2YTaO_6 obtained with $\lambda=0.82465$ Å. The insert highlights the splitting of the $(110)_p$ reflection whilst the change in scale at 50 degrees illustrates the quality of the data and fit to high angles. (b) Neutron powder diffraction profiles for Sr_2YTaO_6 obtained with $\lambda=1.622$ Å. Inset (a) highlights the absence of any obvious splitting of the $(110)_p$ reflection.

Table 1
The structure of Sr_2YTaO_6 as refined from neutron powder diffraction data collected using the Echidna diffractometer at the OPAL facility.

Atom	*x*	*y*	*z*	U_{iso} Å$^2\times10^{-2}$
	T=50 °C, Space group=$P2_1/n$.			
	a=5.8139(3) Å, *b*=5.8578(3) Å, *c*=8.2450(5) Å, β=90.129(6)°, R_p=7.8%, R_{wp}=10.2%, χ^2=1.17			
Sr	−0.0055(14)	0.4694(6)	0.2461(13)	0.41(8)
Y	0	0	0	0.43(12)
Ta	0	0	½	0.48(14)
O1	0.0728(10)	0.0175(9)	0.2640(10)	0.14(11)
O2	0.2247(13)	0.3015(11)	−0.0370(11)	0.16(16)
O3	0.3018(15)	0.7740(16)	−0.0421(11)	1.0 (2)
	T=1000 °C, *Space group=I4/m*. R_p=6.4%, R_{wp}=8.5%, χ^2=1.44			
	a=*b*=5.8866(2), *c*=8.3439(5) Å			
Sr	0	½	¼	4.37(9)
Y	0	0	0	0.4(1)
Ta	0	0	½	2.8(2)
O1	0	0	0.2637(14)	11.3(5)[a]
O2	0.2323(11)	0.2956(12)	0	8.9(2)[b]
	T=1200 °C, *Space Group=Fm3m*			
	a=*b*=*c*=8.3511(2) Å, R_p=6.6%, R_{wp}=8.7%, χ^2=1.49			
Sr	¼	¼	¼	4.79(7)
Y	0	0	0	2.14(11)
Ta	½	½	½	1.55(1)
O1	0.2651(3)	0	0	6.9(1)[c]

[a] $U_{11}=U_{22}=5.5(4)$ Å$^2\times10^{-20}$, $U_{33}=0.29(9)$ Å$^2\times10^{-2}$.
[b] $U_{11}=0.68(14)$ Å$^2\times10^{-20}$, $U_{22}=5.9(4)$ Å$^2\times10^{-20}$, $U_{33}=2.3(1)$ Å$^2\times10^{-20}$, $U_{12}=-1.4(2)$ Å$^2\times10^{-20}$.
[c] $U_{11}=0.41(3)$ Å$^2\times10^{-20}$, $U_{22}=U_{33}=3.22(4)$ Å$^2\times10^{-2}$.

provide evidence for some, local, disorder in the monoclinic structure.

The preparative method alters the local structure of Sr_2YTaO_6, as evident from the present diffraction and Raman results, and may explain the different structures reported for these types of oxides in the literature, especially when it is recalled that many researchers only utilise conventional (Cu$K\alpha$) powder X-ray diffractometers. Data obtained with such an instrument did not reveal the presence of the "second phase" required to reproduce the synchrotron data of the ball-milled sample. In many cases the failure of such methods to detect subtle differences in crystal symmetry possibly reflects the high pseudo-symmetry of perovskites. The differences between the two samples described here are of particular importance for the study of the microwave dielectric properties of such oxides, where the preparation of dense single phase samples is critical. The ball mill method utilised here is commonly employed in such studies, yet this clearly results in samples containing more stacking faults and/or disorder than in the sample prepared using conventional solid state methods, even though the former was ultimately heated to higher temperature.

Portions of the ball-milled sample were then reheated at 1400 °C for 4, 8, 24, and 48 h and their structures examined after each of these heating steps using a conventional X-ray diffractometer. Such heating resulted in an increase in the intensity of the diffracted lines and a slight reduction in the widths of the various peaks. As noted above the resolution of this diffractometer is not sufficient to unequivocally establish the co-existence of the two

Table 2
Bond lengths and bond valence sums (BVS) for the monoclinic, tetragonal, and cubic structures observed in the conventionally prepared Sr_2YTaO_6 sample.

Structure	Sr–O		Y–O		Ta–O	
	Bond length (Å)	BVS	Bond length (Å)	BVS	Bond length (Å)	BVS
$P2_1/n$ 50 °C	O1 2.687(6) O1 2.511(11) O2 2.844(12) O2 2.531(12) O2 2.879(11) O3 2.795(14) O3 2.940(15) O3 2.587(12)[a]	1.69	O1 × 2 2.220(9) O2 × 2 2.216(8) O3 × 2 2.221(8)	3.45	O1 × 2 2.002(8) O2 × 2 2.001(8) O3 × 2 2.006(8)	4.95
$I4/m$ 1000 °C	O1 × 4 2.9456(4) O2 × 4 2.700(4)[a]	1.37	O1 × 2 2.201(12) O2 × 4 2.214(8)	3.54	O1 × 2 1.972(12) O2 × 4 1.983(8)	4.70
$Fm\bar{3}m$ 1200 °C	O1 × 12 2.9554(1)	1.25	O1 × 6 2.212(5)	3.51	O1 × 6 1.964(6)	5.33

[a] There are four longer (> 3.0 Å) Sr–O distances.

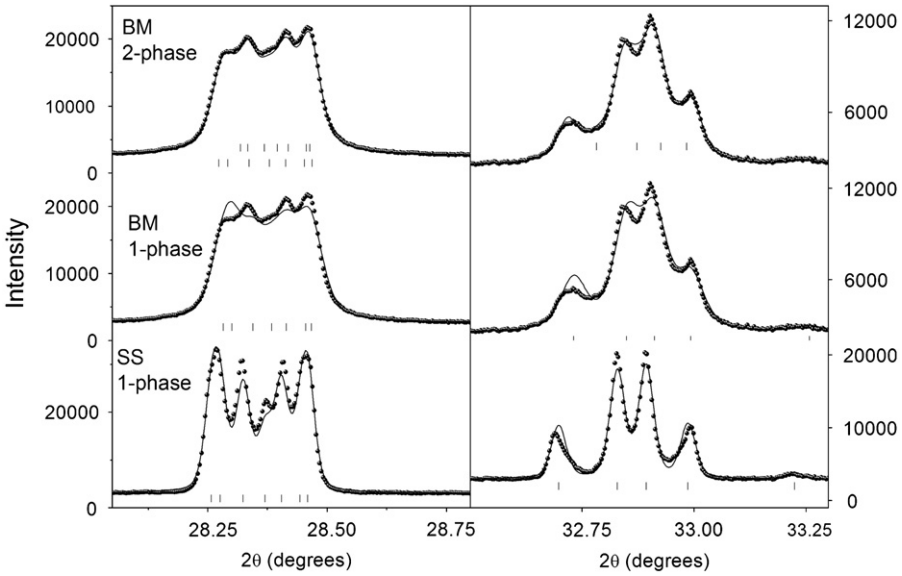

Fig. 2. Sections of the synchrotron diffraction patterns for Sr_2YTaO_6 prepared using ball milling (BM) and conventional solid state (SS) methods. The lines are from Rietveld analysis and highlight the failure of the single phase model to fit the data in the ball milled sample.

Table 3
The room temperature structure of Sr_2YTaO_6 prepared using a ball mill as refined from synchrotron X-ray diffraction data. The unit-cell dimensions are Phase (1) $a=5.81145(4)$ Å, $b=5.85641(4)$ Å, $c=8.24136(5)$ Å, $\beta=90.1479(4)^\circ$ 70.7(5) wt%: Phase (2) $a=5.81272(11)$ Å, $b=5.84750(9)$ Å, $c=8.23703(11)$ Å, $\beta=90.127(1)^\circ$ 29.3 wt%. Both phases are in space-group symmetry $P2_1/n$ and were restrained to have identical atomic coordinates. The measures of fit were R_p 2.6%, R_{wp} 3.6%, χ^2 4.50.

Atom	*x*	*y*	*z*	U_{iso} (Å^2 × 10^{-2})
Sr	−0.0052(3)	0.4687(1)	0.2500(2)	1.69(1)
Y	0	0	0	0.59(1)
Ta	0	0	0.5	0.95(1)
O1	0.0741(12)	0.0146(9)	0.2621(9)	0.86(16)
O2	0.2369(14)	0.2899(12)	−0.0369(13)	0.57(20)
O3	0.3024(14)	0.7762(13)	−0.0389(13)	1.3(9)

phases, but these results strongly suggest that further heating yields a single phase sample. This conclusion is supported by Raman measurements, where the heated samples displayed somewhat sharper lines, and the weak additional features apparent in Fig. 3 were no longer present.

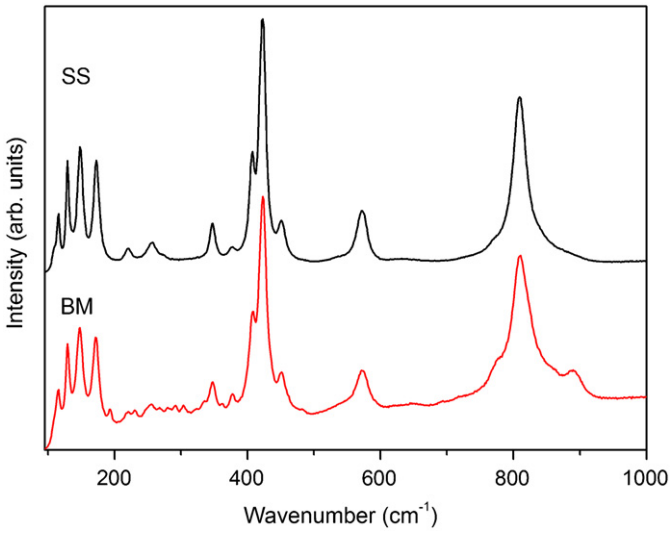

Fig. 3. Sections of the Raman spectra for Sr_2YTaO_6 prepared using ball milling (BM) and conventional solid state (SS) methods. Note the broadening and presence of additional lines in the former sample.

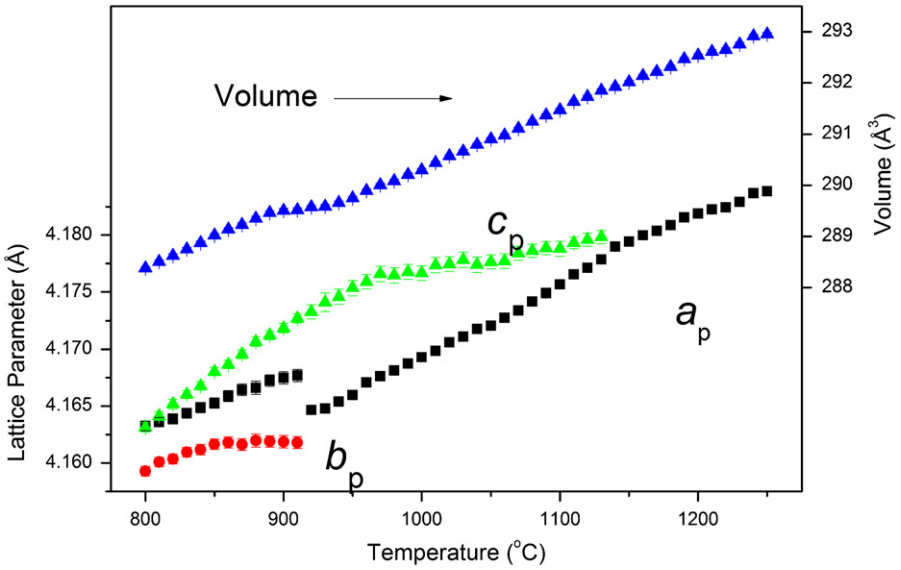

Fig. 4. Evolution of the lattice parameters for Sr_2YTaO_6 between 800 and 1250 °C from variable temperature X-ray diffraction data. There is clear evidence for a first order transition near 930 °C.

Subsequently detailed studies of the structure and phase transitions were limited to the conventionally prepared sample. Although the synchrotron diffraction data showed clearly resolved reflections indicative of monoclinic symmetry the lower resolution of the neutron diffraction data precludes this, as is evident from a comparison of Fig. 1(a) and (b). Nevertheless the greater sensitivity of the neutron data to displacements of the lighter oxygen atoms results in more accurate structural refinements.

Ordering of the Y^{3+} and Ta^{5+} cations in Sr_2YTaO_6 results in the same superlattice reflections as does in-phase tilting of the BO_6 octahedra [7,23]. Out-of-phase-tilting, however, results in the appearance of additional reflections. By comparison with other double perovskite systems including the closely related Ba_2LnNbO_6 (*Ln*—a lanthanide) oxides we anticipate that the out-of-phase tilts will be lost at a lower temperature than the in-phase tilts [12,24]. Variable temperature neutron diffraction patterns demonstrate this to be the case with the strongest *M*-point reflection indicative of out-of-phase tilting lost by 1000 °C. At this point the sample is, within the resolution of the neutron diffraction measurements, metrically cubic. Attempts to refine a structure to a cubic model in $Fm\bar{3}m$ were less than optimal suggesting the symmetry was in fact lower; therefore, we used X-ray diffraction data to establish the symmetry of the intermediate phase(s). These data suggest the presence of two phase transitions; the first near 925 °C is first order and corresponds to a transition to a tetragonal structure in space group $I4/m$. The second near 1150 °C is the transition to the cubic structure. The neutron patterns at 1000 and 1200 °C were fitted to the appropriate models and the results summarised in Table 1.

The thermal evolution of the lattice parameters obtained from the XRD data provides some evidence for a third phase transition near 850 °C, namely the change in the rate of thermal expansion along the *b*-axis at this point (Fig. 4). We postulate that this is due to a transition to a second monoclinic structure in space group $I2/m$. High quality neutron diffraction data would be required to unequivocally establish this; however, based on both our group theoretical analysis [7] and previous experimental studies [24,25] this appears to be a reasonable assertion. The sequence of phase transitions can be understood in terms of the tilting of the BO_6 units. The $P2_1/n$ structure is characterised by both in-phase (or positive) and out-of phase (negative) tilts ($a^-a^-c^+$) with the in-phase tilt about (0 0 1) being lost at the transition to the $I2/m$ structure ($a^-a^-c^0$). The first order $I2/m$ to $I4/m$ transition involves a reorientation of the out-of-phase tilts from about (110) to (001) with the tilt system in this tetragonal structure being $a^0a^0c^-$. Finally, the out-of-phase tilts are lost at the transition to the cubic $Fm\bar{3}m$ structure ($a^0a^0a^0$) [7,26].

A feature of both the tetragonal and cubic structures is the strongly anisotropic nature of the anion displacements, see Table 1. In the case of the cubic $Fm\bar{3}m$ structure, introduction of anisotropic displacement parameters (ADPs) for the anion during the refinement against the neutron diffraction data collected at 1200 °C resulted in a reduction of χ^2 from 2.32 to 1.58. For the tetragonal $I4/m$ structure χ^2 reduced from 1.96 to 1.56 upon the introduction of ADPs for the two anions, when considering the neutron data collected at 1000 °C. The significance of this is evident upon considering the structures. In the case of the cubic structure the displacement is considerably larger towards the cuboctahedral sites occupied by the Sr cations than along the shorter *B*–O bond directions. This anisotropic displacement effectively shortens the *A*–O bonds whilst lengthening the *B*–O bonds in a similar manner to the cooperative tilting of the BO_6 octahedra. A similar phenomenon is observed in the tetragonal structure.

4. Conclusion

The crystal structure of the rock-salt ordered double perovskite Sr_2YTaO_6 has been investigated from room temperature to 1250 °C using neutron and X-ray diffraction data. This oxide exhibits a sequence of phase transitions associated with the removal of the cooperative tilting of the BO_6 octahedral units. The high temperature tetragonal and cubic phases are characterised by strongly anisotropic displacement parameters for the anions. High resolution synchrotron diffraction studies show the crystallinity of the sample is sensitive to the precise method used to prepare the sample.

Acknowledgments

This work was, in part, performed at the powder diffraction beamline at the Australian Synchrotron. BJK acknowledges the support of the Australian Research Council for this work.

References

[1] M.A. Pena, J.L.G. Fierro, Chemical Reviews 101 (2001) 1981–2017.
[2] I.M. Reaney, D. Iddles, Journal of the American Ceramic Society 89 (2006) 2063–2072.
[3] Y.-H. Huang, G. Liang, M. Croft, M. Lehtimaki, M. Karppinen, J.B. Goodenough, Chemistry of Materials 21 (2009) 2319–2326.
[4] O. Chmaissem, B. Dabrowski, S. Kolesnik, J. Mais, D.E. Brown, R. Kruk, P. Prior, B. Pyles, J.D. Jorgensen, Physical Review B 64 (2001) 9.
[5] Y.I. Kim, P.M. Woodward, Journal of Solid State Chemistry 180 (2007) 2798–2807.
[6] P.K. Davies, H. Wu, A.Y. Borisevich, I.E. Molodetsky, L. Farber, Annual Review of Materials Research 38 (2008) 369–401.
[7] C.J. Howard, B.J. Kennedy, P.M. Woodward, Acta Crystallographica Section B—Structural Science 59 (2003) 463–471.
[8] P.K. Davies, J.Z. Tong, T. Negas, Journal of the American Ceramic Society 80 (1997) 1727–1740.
[9] I. Levin, J.Y. Chan, R.G. Geyer, J.E. Maslar, T.A. Vanderah, Journal of Solid State Chemistry 156 (2001) 122–134.
[10] P.W. Barnes, M.W. Lufaso, P.M. Woodward, Acta Crystallographica Section B-Structural Science 62 (2006) 384–396.
[11] M.C.L. Cheah, B.J. Kennedy, Physica B—Condensed Matter 385 (2006) 184–186.
[12] P.J. Saines, B.J. Kennedy, M.M. Elcombe, Journal of Solid State Chemistry 180 (2007) 401–409.
[13] R.B. Macquart, Q.D. Zhou, B.J. Kennedy, Journal of Solid State Chemistry 182 (2009) 1691–1693.
[14] A. Dias, L.A. Khalam, M.T. Sebastian, M.M. Lage, F.M. Matinaga, R.L. Moreira, Chemistry of Materials 20 (2008) 5253–5259.
[15] K.D. Liss, B. Hunter, M. Hagen, T. Noakes, S. Kennedy, Physica B Condensed Matter 385–386 (2006) 1010–1012.
[16] K.S. Wallwork, B.J. Kennedy, D. Wang, AIP Conference Proceedings 879 (2007) 879–882.
[17] B.A. Hunter, C.J. Howard, in: A Computer Program for Rietveld Analysis of X-Ray and Neutron Powder Diffraction Patterns Lucas Heights Research Laboratories, Sydney, 1998, pp. 1–27.
[18] C.J. Howard, P.W. Barnes, B.J. Kennedy, P.M. Woodward, Acta Crystallographica Section B-Structural Science 61 (2005) 258–262.
[19] N. Menendez, M. Garcia-Hernandez, D. Sanchez, J.D. Tornero, J.L. Martinez, J.A. Alonso, Chemistry of Materials 16 (2004) 3565–3572.
[20] V. Ting, Y. Liu, R.L. Withers, L. Noren, M. James, J.D.F. Gerald, Journal of Solid State Chemistry 179 (2006) 551–562.
[21] A. Dias, L.A. Khalam, M.T. Sebastian, C. William, C.W.A. Paschoal, R.L. Moreira, Chemistry of Materials 18 (2006) 214–220.
[22] A. Dias, R.G. Sa, R.L. Moreira, Journal of Raman Spectroscopy 39 (2008) 1805–1810.
[23] Q.D. Zhou, B.J. Kennedy, M. Avdeev, L. Giachini, J.A. Kimpton, Journal of Solid State Chemistry 182 (2009) 3195–3200.
[24] P.J. Saines, J.R. Spencer, B.J. Kennedy, M. Avdeev, Journal of Solid State Chemistry 180 (2007) 2991–3000.
[25] P.J. Saines, B.J. Kennedy, B. Johannessen, S. Poulton, Journal of Solid State Chemistry 181 (2008) 2994–3004.
[26] A.M. Glazer, Acta Crystallographica Section B 28 (1972) 3384–3392.